Genes and Pathways Promoting Long-Term Liver Repopulation by *Ex Vivo* hYAP-ERT2 Transduced Hepatocytes and Treatment of Jaundice in Gunn Rats

Esther A. Peterson,[1]* Zsuzsanna Polgar,[1]* Gnanapackiam S. Devakanmalai,[1] Yanfeng Li,[1] Fadi L. Jaber,[1] Wei Zhang,[2] Xia Wang,[1] Niloy J. Iqbal,[3] John W. Murray,[4] Namita Roy-Chowdhury,[1,5] Wilber Quispe-Tintaya,[5] Alexander Y. Maslov,[5] Tatyana L. Tchaikovskaya,[1] Yogeshwar Sharma,[1] Leslie E. Rogler,[1] Sanjeev Gupta,[1,6] Liang Zhu,[1,3] Jayanta Roy-Chowdhury [ID],[1,5] and David A. Shafritz[1,6,7]

Hepatocyte transplantation is an attractive alternative to liver transplantation. Thus far, however, extensive liver repopulation by adult hepatocytes has required ongoing genetic, physical, or chemical injury to host liver. We hypothesized that providing a regulated proliferative and/or survival advantage to transplanted hepatocytes should enable repopulation in a normal liver microenvironment. Here, we repopulated livers of DPPIV⁻ (dipeptidyl peptidase-4) rats and *Ugt1a1* (uridinediphosphoglucuronate glucuronosyltransferase 1a1)-deficient Gunn rats (model of Crigler-Najjar syndrome type 1), both models without underlying liver injury, for up to 1 year by transplanting lenti-hYAP-ERT2 (mutated estrogen receptor ligand-binding domain 2)-transduced hepatocytes (YAP-Hc). Yap (yes-associated protein) nuclear translocation/function in YAP-Hc was regulated by tamoxifen. Repopulating YAP-Hc and host hepatocytes were fluorescence-activated cell sorting–purified and their transcriptomic profiles compared by RNAseq. After 1 year of liver repopulation, YAP-Hc clusters exhibited normal morphology, integration into hepatic plates and hepatocyte-specific gene expression, without dysplasia, dedifferentiation, or tumorigenesis. RNAseq analysis showed up-regulation of 145 genes promoting cell proliferation and 305 genes suppressing apoptosis, including hepatocyte growth factor and connective tissue growth factor among the top 30 in each category and provided insight into the mechanism of cell competition that enabled replacement of host hepatocytes by YAP-Hc. In Gunn rats transplanted with YAP-Hc+tamoxifen, there was a 65%-81% decline in serum bilirubin over 6 months versus 8%-20% with control-Hc, representing a 3-4-fold increase in therapeutic response. This correlated with liver repopulation as demonstrated by the presence of *Ugt1a1*-positive hepatocyte clusters in livers and western blot analysis of tissue homogenates. *Conclusion:* Tamoxifen-regulated nuclear translocation/function of hYAP-ERT2 enabled long-term repopulation of DPPIV⁻/⁻ and Gunn rat livers by hYAP-ERT2-transduced hepatocytes without tumorigenesis. This cell transplantation strategy may offer a potential therapy for most of the inherited monogenic liver diseases that do not exhibit liver injury. (*Hepatology Communications* 2019;3:129-146).

Liver transplantation has markedly improved survival in patients with acute liver failure, end-stage liver disease, and inherited metabolic liver diseases.[(1)] As liver transplantation involves major surgery and is limited by donor organ shortage, transplantation of isolated primary hepatocytes

has been evaluated as a minimally invasive alternative to whole-organ transplantation.[2] Although modest amelioration of several monogenic liver diseases by hepatocyte transplantation has been reported, the number of hepatocytes that can engraft in the liver after introduction into the portal venous system is limited and unmodified adult primary hepatocytes do not proliferate significantly in uninjured host livers.[3,4] However, engrafted hepatocytes can proliferate extensively in genetically manipulated animals, such as urokinase plasminogen activator–transgenic[5] or Fah$^{-/-}$ (fumarylacetoacetate-hydrolase knockout) mice[6] in which there is massive and continuous death of host hepatocytes, which provides a proliferative stimulus to transplanted wild-type (WT) hepatocytes. Less severe chronic hepatocellular stress also provides a proliferative advantage to transplanted cells, as observed in PiZ (alpha-1 antitrypsin Z protein) mice that are transgenic for a misfolded human α_1-antitrypsin variant[7] and the Long-Evans Cinnamon rat model of Wilson's disease.[8] However, in most monogenic liver diseases, such as Crigler-Najjar syndrome type 1 (CN1), ornithine transcarbamylase deficiency, familial hypercholesterolemia, phenylketonuria, and coagulation factors VII and IX deficiency, there is no significant liver injury, whereby transplanted hepatocytes have no proliferative advantage over host hepatocytes and the mass of integrated hepatocytes remains insufficient to cure the disease.

Prolonged genotoxic injury of host liver induced by plant alkaloids, such as retrorsine[3] or monocrotaline[9] or hepatic X-irradiation[4] together with proliferative stimuli, such as partial hepatectomy or liver growth factors like hepatocyte growth factor (HGF), permits extensive repopulation by transplanted hepatocytes. We hypothesized that competitive liver repopulation could also occur if engrafted hepatic cells possessed cell-intrinsic proliferative and/or survival advantage

ARTICLE INFORMATION:

From the [1]Department of Medicine, Marion Bessin Liver Research Center, Albert Einstein College of Medicine, Bronx, NY; [2]Department of Radiation Oncology, Marion Bessin Liver Research Center, Albert Einstein College of Medicine, Bronx, NY; [3]Department of Developmental and Molecular Biology, Marion Bessin Liver Research Center, Albert Einstein College of Medicine, Bronx, NY; [4]Department of Anatomy and Structural Biology, Marion Bessin Liver Research Center, Albert Einstein College of Medicine, Bronx, NY; [5]Department of Genetics, Albert Einstein College of Medicine, Bronx, NY; [6]Department of Pathology, Albert Einstein College of Medicine, Bronx, NY; [7]Department of Cell Biology, Albert Einstein College of Medicine, Bronx, NY.

ADDRESS CORRESPONDENCE AND REPRINT REQUESTS TO:

Jayanta Roy-Chowdhury, M.D.
Department of Medicine, Marion Bessin Liver Research Center
Albert Einstein College of Medicine
1300 Morris Park Avenue
Bronx, NY 10461
E-mail: jayanta.roy-chowdhury@einstein.yu.edu
Tel: +1-718-430-2265
Fax: +1-718-430-8975
or

David A. Shafritz, M.D.
Department of Medicine, Marion Bessin Liver Research Center
Albert Einstein College of Medicine
1300 Morris Park Avenue
Bronx, NY 10461
E-mail: david.shafritz@einstein.yu.edu
Tel: +1-718-430-2125
Fax: +1-718-430-8975

over host cells. We demonstrated this by transplanting isolated fetal liver stem/progenitor cells into normal adult livers.[10] Subsequently, we enhanced liver repopulation by adult hepatocytes transduced *ex vivo* with lentivirus transthyretin (TTR) human *YAP1* fused with a modified ERT2 (mutated estrogen receptor ligand-binding domain 2) before transplantation.[11]

YAP (yes-associated protein) regulates liver size by promoting cell proliferation and inhibiting apoptosis.[12,13] In resting cells, YAP localizes in the cytoplasm, where it undergoes phosphorylation-dependent degradation through Hippo signaling. When the Hippo pathway is turned off by cell proliferative signals, YAP translocates to the nucleus, where it binds to and activates TEADs (TEA domain family members 1-4 transcription factors).[12,13] The hYAP1-ERT2 fusion protein remains in the cytoplasm, but following tamoxifen administration, it translocates to the nucleus,[11] where it binds to TEADs, activating its transcriptional function. As increased proliferative potential of transplanted cells raises concerns of cancer risk, we engineered this system so that the nuclear transcription/activity of YAP could be tightly controlled by tamoxifen administration.

To determine the duration and extent of liver repopulation by hepatocytes lentivirally transduced with hYAP-ERT2 (YAP-Hc) and to elucidate its molecular underpinnings, we transplanted YAP-Hc from dipeptidyl peptidase IV⁺ F344 rats (DPPIV⁺/⁺) into congenic DPPIV⁻/⁻ recipients and used RNAseq with isolated YAP-Hc and host Hc from repopulated rat livers at 1 year to identify specific genes and pathways promoting liver repopulation. To evaluate whether this repopulation strategy can be used to treat an animal model of a human metabolic liver disease with no underlying liver injury, we transplanted WT Wistar-RHA (Roman high-avoidance) rat YAP-Hc into *Ugt1a1* (uridinediphosphoglucuronate glucuronosyltransferase 1a1)-deficient jaundiced Gunn rats, a model of CN1, and showed progressive and marked reduction of serum bilirubin following liver repopulation.

Materials and Methods

ANIMALS

Inbred Wistar-RHA rats congenic with *Ugt1a1*-deficient Gunn rats were maintained in the Animal Models, Stem Cells, and Cell Therapy Core of the Liver Research Center. Inbred DPPIV⁺ F344 rats, purchased from Taconic Farms (Germantown, NY), were used as hepatocyte donors for DPPIV⁻/⁻ F344 rats. All procedures were approved by the Institutional Animal Care and Use Committee, Albert Einstein College of Medicine, and were carried out in a humane manner in accordance with approved guidelines. Rats were fed a diet containing 400 mg/kg tamoxifen citrate prepared by Bio-Serve (Frenchtown, NJ) or normal rodent chow, as indicated. Animals receiving tamoxifen did not show histological evidence of liver injury.

HEPATOCYTE ISOLATION, RECOMBINANT LENTIVIRUS PRODUCTION, LENTIVIRAL TRANSDUCTION OF PRIMARY RAT HEPATOCYTES, RNA ISOLATION, REAL-TIME POLYMERASE CHAIN REACTION, AND QUANTITATIVE REAL-TIME POLYMERASE CHAIN REACTION

All procedures were performed as previously reported.[11]

GUNN RATS: EXPERIMENTAL GROUPS

Adult (200 g) Gunn rats of both genders were subjected to 66% hepatectomy and stratified into various experimental groups described in Fig. 7A and the Supporting Information.

STAINING OF LIVER SECTIONS

Procedures for hematoxylin and eosin (H&E) staining, immunofluorescent and immunohistochemical staining, and histochemical staining for DPPIV and γ-glutamyl transpeptidase (GGT) are described in the Supporting Information.

FLUORESCENCE-ACTIVATED CELL SORTING

To separate host DPPIV⁻/⁻ liver hepatocytes from hepatocytes derived from transplanted DPPIV⁺ donor

cells, we performed fluorescence-activated cell sorting (FACS) using two antibodies: (1) anti-DPPIV mouse monoclonal antibody (Santa Cruz Biotechnology Inc., Dallas, TX) plus secondary goat anti-mouse-Alexa 488 conjugated antibody (Jackson lmmunoResearch Laboratories, West Grove, PA), and (2) phycoerythrin-conjugated anti-ICAM antibody to identify hepatocytes (Invitrogen, Thermo Fisher Scientific). Isotype-matched irrelevant (control) antibodies were used to determine background staining. Fifty thousand cells were sorted into two groups: ICAM⁺/DPPIV⁺ (ID) repopulating hepatocytes and ICAM⁺/DPPIV⁻ (I) host hepatocytes. FACS-purified hepatocytes were immersed into Qiazol for RNA extraction (Supporting Information).

RNA PREPARATION FOR SEQUENCING OF TRANSCRIPTOME RNA LIBRARIES, SEQUENCE DATA ACQUISITION, PROCESSING, AND ANALYSIS

See Supporting Information.

PLOIDY ANALYSIS

To determine the ploidy state of repopulating YAP-Hc and host hepatocytes, we analyzed the DNA content with Hoechst 33258 dye staining in tissue sections from 3 rats at 1 year after cell transplantation (Supporting Information).

STATISTICS

Data are shown as mean ± SEM. Statistical significance was determined by a two-tailed Student t test.

Results

YAP-Hc PROGRESSIVELY REPOPULATE THE LIVER OF DPPIV⁻ F344 RECIPIENTS FOR 12 MONTHS

The duration and extent of liver repopulation by YAP-Hc was determined in DPPIV⁻ rats (Fig. 1A) with tamoxifen administration continuously in the

food for up to 12 months. As shown by DPPIV enzyme histochemistry, the number of DPPIV⁺ clusters were similar at 6 and 12 months, but repopulating clusters was much larger at 12 months (Fig. 1B, left panels). Morphometric quantification showed 3.56% ± 0.90% and 13.84% ± 2.80% hepatocyte replacement at 6 and 12 months, respectively (Fig. 1B, middle panel), representing a 4-fold increase at 12 months (P = 0.024) and no reduction in liver repopulation when tamoxifen feeding was discontinued during the second 6 months after YAP-Hc transplantation (Fig. 1B, right panel).

LIVER MORPHOLOGY REMAINED NORMAL AFTER YAP-Hc/TAMOXIFEN-INDUCED LIVER REPOPULATION

H&E staining and DPPIV/YAP immunohistochemistry after 12 months of repopulation showed normal liver lobular structure (Fig. 1C). YAP-Hc were fully integrated into hepatic parenchyma without compressing or distorting the surrounding liver tissue. Donor cell clusters were indistinguishable from host hepatocytes, except for DPPIV and YAP expression (Fig. 1C,D) and showed normal cell surface membrane polarity (i.e., DPPIV expression on the apical domain and either Ntcp [sodium taurocholate cotransporter protein] [Fig. 1E] or Oatp1a1 [organic anion transport protein 1a1] [Fig. 1F]) on the baso-lateral domain of transplanted cells. Repopulating YAP-Hc and host hepatocytes were oriented in the same direction in the parenchymal plates, as demonstrated by the pattern of green immunostaining in the baso-lateral domain of both cell types, better illustrated with Ntcp (Fig. 1E).

PLOIDY STATE OF REPOPULATING YAP-HC WAS SIMILAR TO THAT OF HOST HEPATOCYTES

Analysis of DNA content of both YAP-Hc and host hepatocytes in same tissue sections (Fig. 2A) from 3 rats 1 year after cell transplantation showed that 2N(diploid), 4N(tetraploid), and 8N+(octaploid) classes were similar for donor and host hepatocytes: 35% versus 35%, 55% versus 57%, and 9% versus 7%,
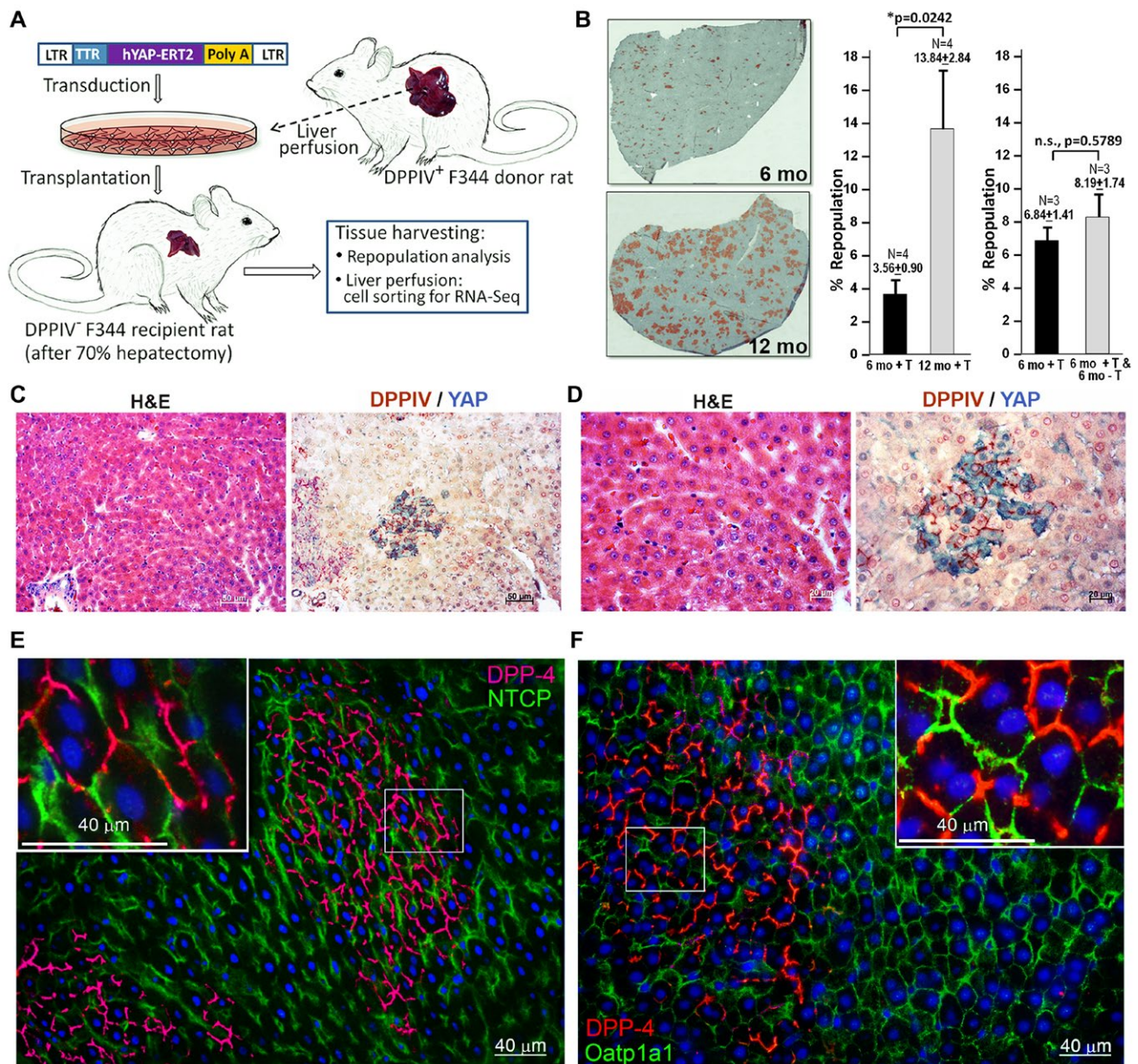
FIG. 1. Repopulation of normal rat liver by lenti-TTR-hYAP-ERT2-transduced hepatocytes 1 year after cell transplantation. (A) Schematic diagram of hepatocyte transplantation protocol. (B) Detection of WT DPPIV⁺ repopulating hepatocyte clusters in DPPIV⁻ recipients by enzyme histochemistry. (C,D) Analysis of consecutive sections by H&E staining and DPPIV/Yap immunohistochemistry 1 year after cell transplantation (C = ×10 magnification; D = ×40 magnification). (E,F) Demonstration of hepatocyte cell-surface membrane polarity and orientation of transplanted cells in the parenchymal plates using double-label immunohistochemistry for DPPIV and Ntcp (E) or Oatp1a1 (F). Abbreviations: LTR, long terminal repeat.

respectively ($P > 0.99$) (Fig. 2B). Modal DNA content across these ploidy classes was also similar (Fig. 2C-E). This analysis did not show emergence of new subclasses with intermediate DNA content within diploid (2-3.9N), tetraploid (4-7.9N), or octaploid (8-16N) classes in repopulating YAP-Hc, indicating that there was no increase in aneuploidy in transplanted hepatocytes over neighboring host hepatocytes.
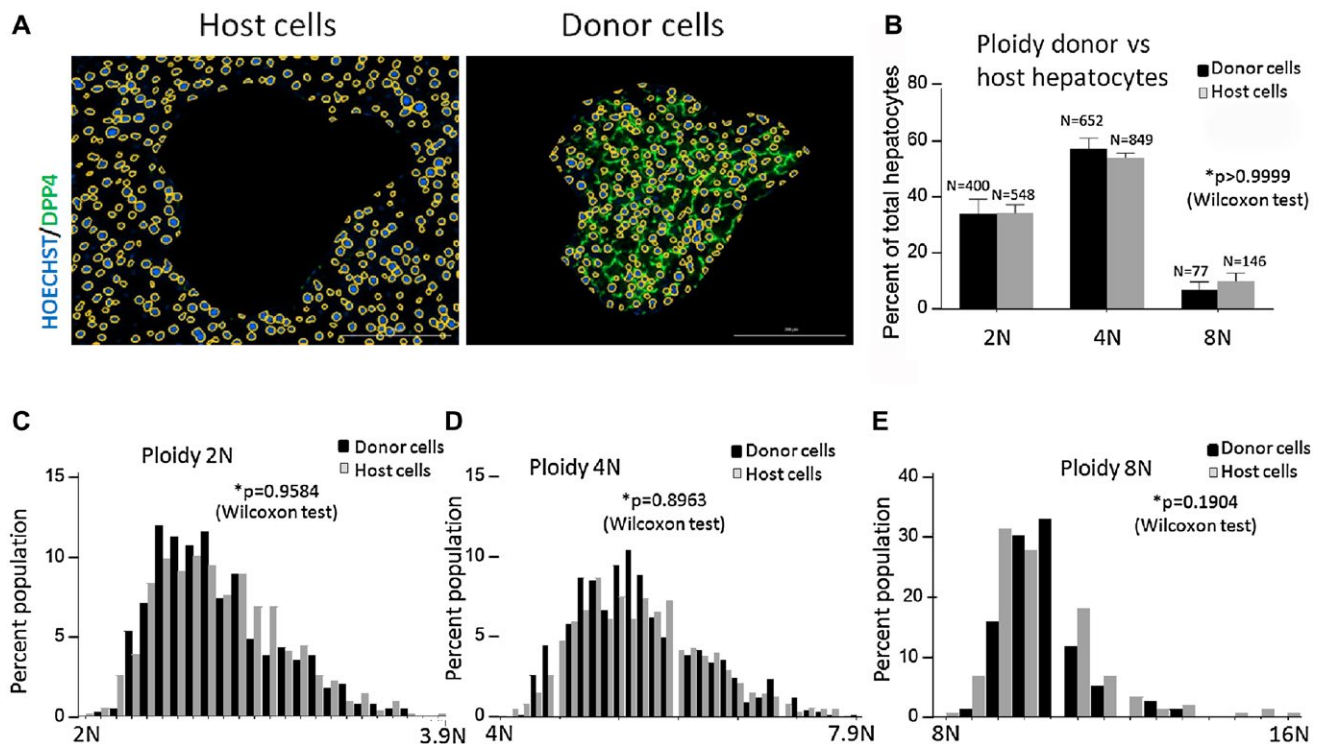
FIG. 2. Ploidy class distribution at 1 year in YAP-Hc and host hepatocytes. (A) Staining of nuclei in 5-um tissue sections with Hoechst 33258 dye (blue) and the cell surface of transplanted YAP-Hc with DPPIV antibody (green). (B) Ploidy classes in YAP-Hc and host hepatocytes (n = 3 rats) were similarly distributed (n = number of hepatocytes counted; black bars = donor [DPPIV$^+$] cells; gray bars = host [DPPIV$^-$] cells). *P* values were determined by Wilcoxon rank sum test. (C-E) Ploidy distribution profiles in 2N, 4N, and 8+N cell populations showed no statistically significant difference in modal DNA content in YAP-Hc versus host hepatocytes in these three subclass populations. Therefore, new subclasses with intermediate DNA content were not observed in YAP-Hc.

REPOPULATING CLUSTERS EXPRESS HEPATOCYTE-SPECIFIC PROTEINS, BUT NOT MARKERS OF HEPATIC PROGENITORS, BILIARY EPITHELIUM, OR HEPATOCELLULAR CARCINOMA

Immunofluorescence staining of liver sections 12 months after YAP-Hc transplantation showed that DPPIV$^+$ clusters were positive for YAP and hepatocyte-specific proteins (albumin, HNF4α, and asialoglycoprotein receptor) (Fig. 3A). In contrast, markers of hepatic progenitor cells or biliary epithelial cells (CK-19, SOX9, and EpCAM) or hepatocellular carcinoma (Afp, CD133, and CD44) were undetectable in hepatocytes (Fig. 3A). Vimentin-positive cells were equally distributed in host liver and repopulating DPPIV$^+$ cluster regions, but YAP-Hc were vimentin-negative. YAP-Hc were also negative for desmin

and α-smooth muscle actin, indicating absence of epithelial-mesenchymal transition (EMT).

NO LIVER FIBROSIS OR FOCAL NODULAR TRANSFORMATION OF DONOR HEPATOCYTE CLUSTERS

H&E, trichrome, and sirius red staining in consecutive sections of liver 12 months after cell transplantation showed normal liver histology and no evidence of fibrosis in recipient liver or DPPIV$^+$ clusters (Fig. 3B). Staining for GGT that is normally expressed in bile duct epithelial cells and is a classic marker for focal nodular transformation of hepatocytes,[14] and DPPIV by enzyme histochemistry in serial sections showed that host bile duct epithelial cells stained positive for GGT, but YAP-Hc clusters were negative (Fig. 3C). Taken together, data in Figs. 2 and 3 indicate that repopulating YAP-Hc clusters exhibit
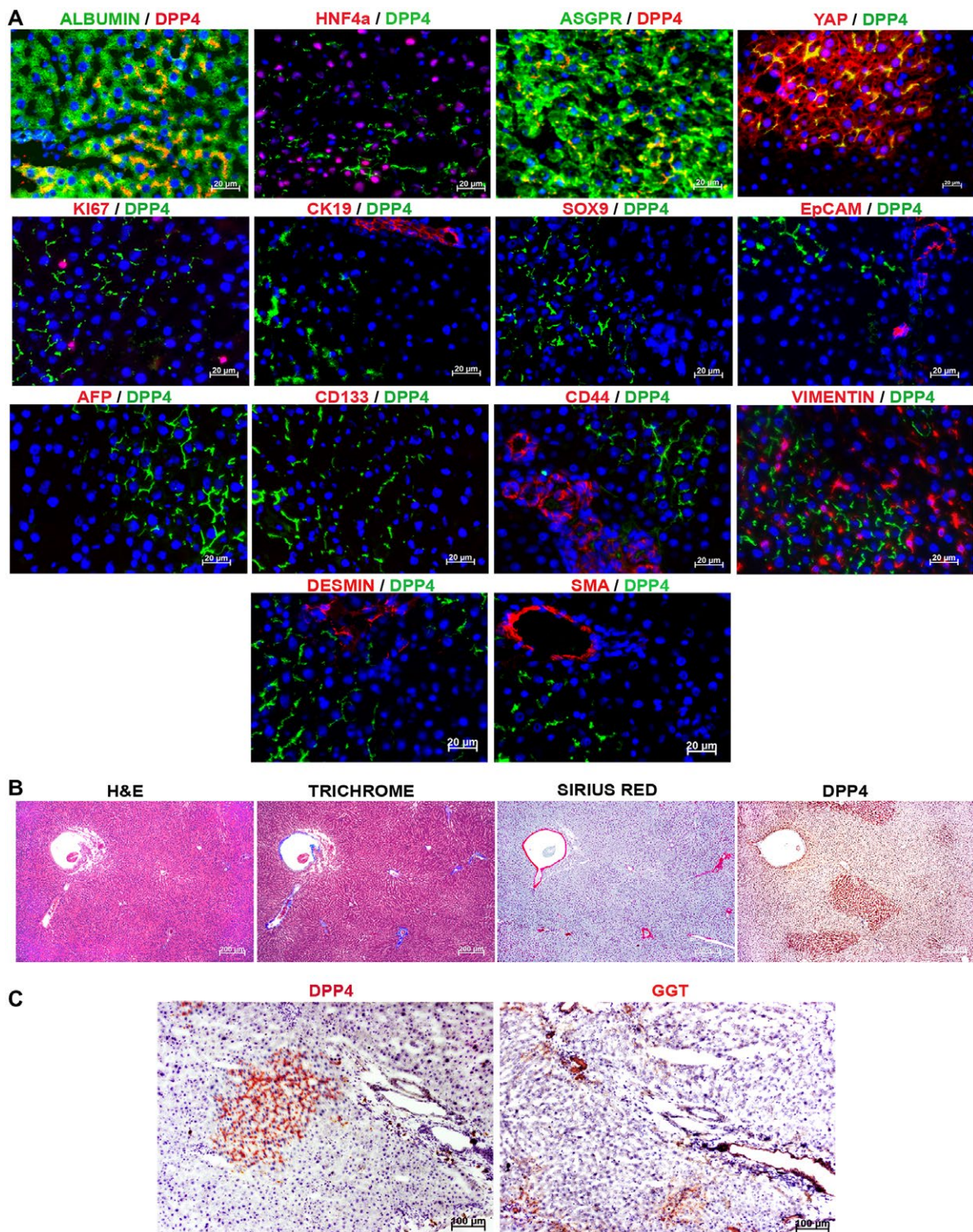
FIG. 3. Histochemical analysis of liver tissue 1 year after cell transplantation for hepatic gene expression. (A) The specific protein paired with DPPIV and the fluorescent color generated by second antibody are given for each panel. (B) Histochemical analysis of YAP-Hc transplanted tissue for hepatic fibrosis by H&E, trichrome, and sirius red staining. (C) DPPIV and GGT staining in consecutive sections of rat liver 1 year after YAP-Hc transplantation, showing GGT staining of bile duct epithelial cells and scattered cells in hepatic parenchyma. All hepatocytes in DPPIV$^+$ clusters are GGT negative and all bile ducts are DPPIV negative.

a normal mature hepatocyte phenotype, without evidence of dysplasia, dedifferentiation, transdifferentiation, EMT, or preneoplastic transformation 1 year after cell transplantation.

CELL COMPETITION BETWEEN YAP-Hc AND HOST HEPATOCYTES

Immunofluorescent staining for Ki-67, a cell proliferation marker, showed that at both 6 and 12 months after cell transplantation, the proliferation rate was approximately 3-fold higher in YAP-Hc-derived DPPIV[+] clusters, compared with surrounding host hepatocytes ($P = 0.002$ and $P = 0.02$, respectively) (Fig. 4A-D). In contrast, 3-fold to 4-fold fewer cells in repopulating clusters were engaged in apoptosis compared with host hepatocytes (shown by staining for active caspase-3) at 6 months ($P = 0.008$) and 12 months ($P = 0.04$) (Fig. 4E-H). (See Supporting

Table S1 for numbers of animals used, cells counted for Ki67 and active caspase-3, and percentage of total cells in each category.) These differences in proliferation and apoptosis of YAP-Hc versus host hepatocytes at both 6 months and 12 months indicate a cell competition-like mechanism.[15]

GENOME-WIDE TRANSCRIPTOME ANALYSIS OF YAP-Hc VERSUS HOST HEPATOCYTES

Hepatocytes isolated from repopulated livers at 3 months and 6 months following transplantation were FACS-purified into I-CAM1^{+}/DPPIV[−] host hepatocytes (I) and I-CAM1^{+}/DPPIV[+] repopulating YAP-Hc (ID) and showed total separation of these two cell populations (Fig. 5A). Using RNAseq, we compared normalized read counts from 4 donor/recipient pairs isolated at 3 months and 6 months,
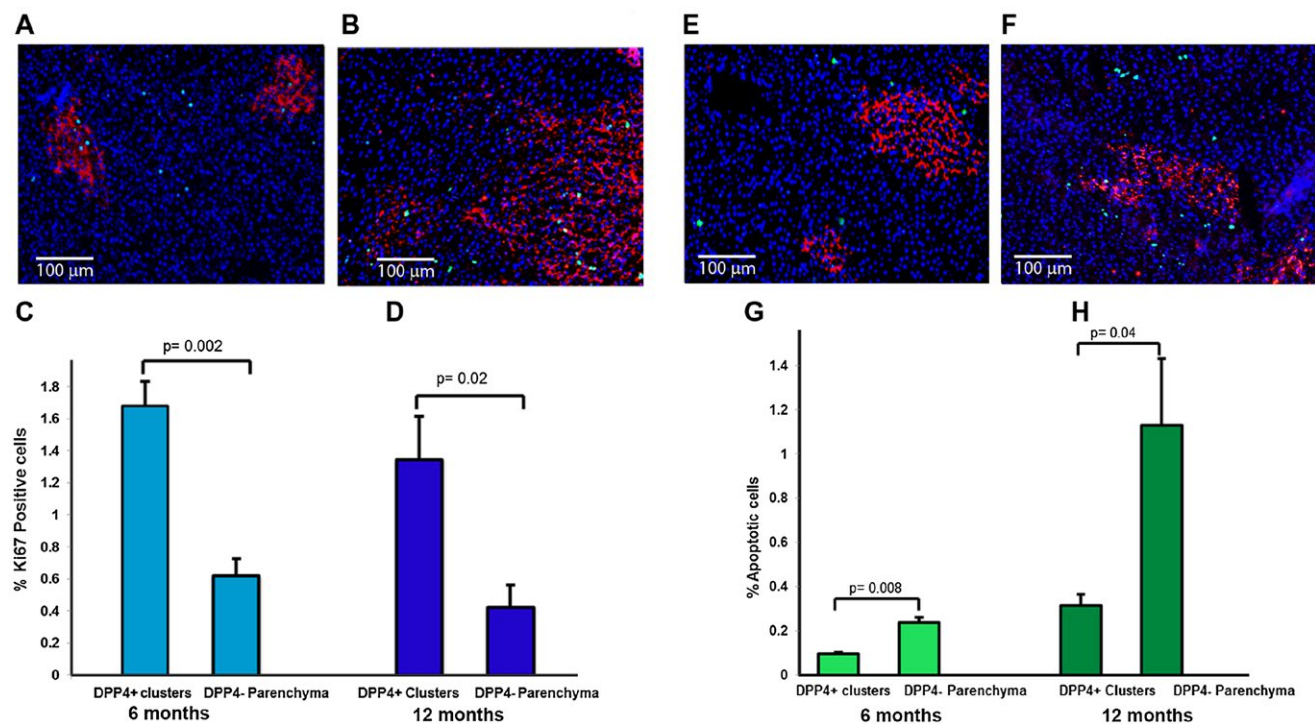

FIG. 4. Detection and quantification of proliferating and apoptotic transplanted versus host hepatocytes by fluorescent immunohistochemistry for Ki67 and active caspase-3. (A,B) Merged immunofluorescent images for DPPIV (red) and Ki67 (green) at 6 months (A) and 12 months (B) (blue = nuclei stained with DAPI [4′,6-diamidino-2-phenylindole]). (C,D) Quantification of proliferating (Ki67^{+}) hepatocytes in DPPIV[+] repopulating clusters and DPPIV[−] host hepatocytes by Image J analysis at 6 months and 12 months after cell transplantation. (E,F) Merged immunofluorescent images for DPPIV (red) and active caspase-3 (green) at 6 months (E) and 12 months (F) after cell transplantation. (G,H) The percentage of apoptotic cells was about 3-fold higher in DPPIV[−] host hepatocytes compared with DPPIV[+] transplanted hepatocytes at both 6 months (G) and 12 months (H). *P* values for (C), (D), (G), and (H) were determined by two-tailed Student *t* test.
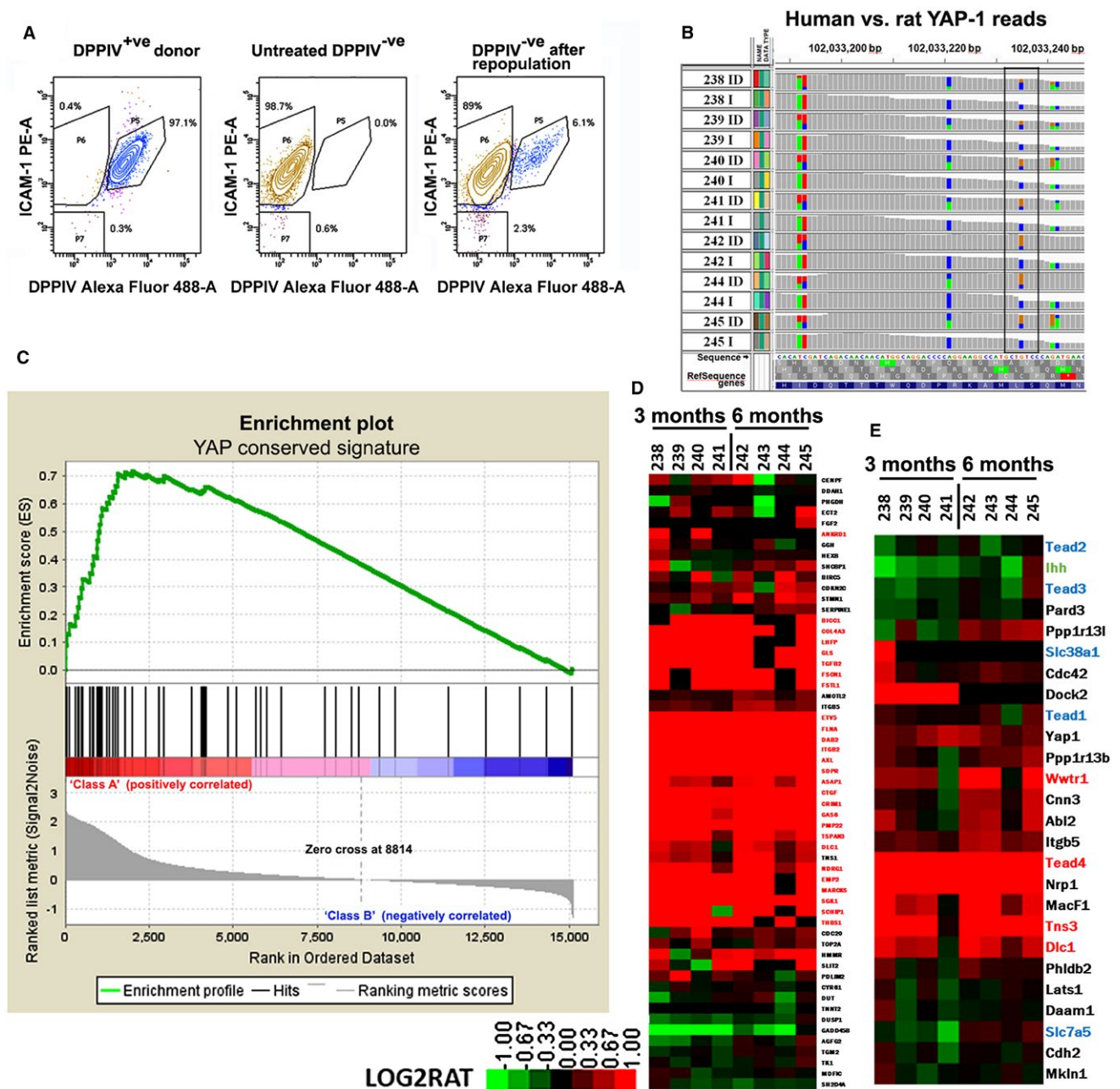
FIG. 5. RNAseq analysis of FACS-sorted YAP-Hc and host hepatocytes. (A) FACS: Hepatocytes were isolated according to positivity for ICAM-1 (marker for all hepatocytes) and DPPIV (marker for donor hepatocyte). P5, ICAM-1$^+$/DPPIV$^+$: left panel, donor hepatocytes; right panel, donor progeny in 6-month repopulated liver. P6, ICAM-1$^+$/DPPIV$^-$: middle panel, host hepatocytes; right panel, host hepatocytes in 6-month repopulated liver; left panel, hepatocytes from DPPIV$^+$ donor rat. (B) Integrative Genomic Viewer display of reads mapping to YAP1. Read counts from individual RNAseq libraries are displayed for ICAM$^+$/DPPIV$^+$ (ID) and ICAM$^+$/DPPIV$^-$ (I) hepatocyte pairs. The human *YAP1* sequence is displayed. Nucleotide color code: A, green; T, red; C, blue; G, umber. Sequence locations exhibiting a difference between human *YAP1* and rat *Yap1* are highlighted. In the boxed nucleotide position, the rat nucleotide is C = blue, whereas the human nucleotide is G = umber. (C) GSEA plot of YAP-conserved signature in RNAseq data from ICAM$^+$/DPPIV$^+$ (ID) and ICAM$^+$/DPPIV$^-$ (I) pairs. (D) Clustergram of the log2RAT ID/I in the 8 donor/host pairs for genes contained in the YAP-conserved signature. (E) Clustergram displaying the log2 RAT ID/I for genes known to be downstream of YAP activation. Significantly up-regulated genes are marked red, unregulated genes are marked blue, down-regulated genes are marked green, and inconsistent changes between 3-month and 6-month samples are marked black.

respectively. Both YAP-Hc (ID) and host (I) populations showed typical hepatocyte gene-expression profiles with albumin messenger RNA expressed at the highest level (Supporting Table S2). Using the Integrative Genomics Viewer (Broad Institute, Cambridge, MA), specific expression of hYAP1 was identified by comparing the read counts in regions of the *YAP* gene, in which there are single nucleotide differences between human and rat *Yap* (Fig. 5B). hYAP sequences were found only in ICAM+/DPPIV+ (ID) cells (Fig. 5B). For example, in the boxed region of Fig. 5B, all YAP-Hc (ID) preparations showed both the human nucleotide G (umber) and rat nucleotide C (blue) at this position, whereas all host hepatocyte preparations (I) showed only rat nucleotide C (blue). Similar results were obtained for hERT2 versus rat ESR1 (estrogen receptor 1) reads at specific locations where nucleotide changes were observed (Supporting Fig. S1).

To determine whether hYAP-ERT2 transgene expression altered endogenous gene expression, we compared the normalized read count obtained by the RNA-seq of YAP-Hc to that of host hepatocytes. Of the 2,080 significantly regulated genes in YAP-Hc in all 8 donor/recipient pairs ($P \leq 0.001$), 2,026 were up-regulated and 55 genes were down-regulated (Supporting Fig. S2). Supporting Table S3 lists all significantly regulated genes and their relative regulation. We used the Gene Set Enrichment Analysis (GSEA, Broad Institute)[16,17] to determine whether known YAP targets were induced in YAP-Hc. Of the two published YAP target gene signatures, YAP1 UP[18] and YAP/TAZ conserved,[19] our Yap signature best matched the latter (normalized enrichment score = 1.81, false discovery rate q value = 0.001) (Fig. 5C). Twenty-seven of the 50 genes in the YAP/TAZ conserved signature were significantly up-regulated in YAP-Hc ($P \leq 0.001$) (Fig. 5D, red letters).

To understand how YAP expression alters the molecular and cellular behavior of YAP-Hc, we queried RNAseq data for regulated expression of YAP/TAZ transcriptional co-activators and downstream effectors in YAP-Hc (Fig. 5E). WWTR (Taz) was up-regulated 1.9 fold at 6 months. YAP1 and WWTR1 bind to TEADs. TEADs 1, 2, and 3 were not significantly regulated in YAP-Hc. Binding of Yap/Taz to *Tead1* increases expression of amino acid transporters, *Slc7a5* and *Slc38a1*, which are essential for mTorc-mediated growth regulation and participate

in hepatocarcinogenesis.[20,21] However, *Slc7a5* and *Slc38a1* were not up-regulated in YAP-Hc (Fig. 5E). It has also been reported that increased WWTR1 expression induces Indian hedgehog (IHH), which leads to increased inflammation and hepatic fibrosis.[22] Interestingly, IHH expression was decreased in YAP-Hc (Fig. 5E), at the borderline of statistical significance ($P = 0.053$).

Tead4 expression was up-regulated 12.4-fold in YAP-Hc (Fig. 5E). *Tead4* is part of a cascade that leads to activation of *Dlc1*, a potent tumor suppressor that inhibits cell growth and tumorigenicity in hepatocellular carcinoma cells.[23] *Dlc1* has RhoGAP (GTPase activating protein) activity, which suppresses cell growth and directional migration during development.[24] Yap/*Tead4*, in concert with *Ap1*, induces *Tns3*, which binds to and activates *Dlc1* to inhibit Rhoa as part of its tumor suppressor function.[23,24] *Tns3* and *Dlc1* are significantly up-regulated in YAP-Hc (2.77 fold and 1.56 fold, respectively) (Fig. 5E). By comparing our data to the cancer genome landscape,[25] we identified five other tumor suppressors that are significantly up-regulated in YAP-Hc: *Prdm1*, *Kdm6a*, *Tnfa1p3*, *Atm*, and *Msh2* (Supporting Table S3). We used GSEA to generate a gene signature for YAP-Hc (Fig. 6A). The top 50 up-regulated genes in this signature included four known Yap targets: *Emp2*, *Dab2*, *Tead4*, and *Marcks*. Among the top 50 down-regulated genes in YAP-Hc (Fig. 6A) are *LGR5*, a marker of a progenitor phenotype,[26] and *Prom1* (CD133), a known tumor progenitor cell gene.[27]

We used the phenotype prediction analysis algorithm of Ingenuity Pathway Analysis (IPA) to gain an understanding of cellular processes affected by tamoxifen-induced hYAP expression in YAP-Hc. We found 145 genes that promote cell proliferation are up-regulated in repopulating YAP-Hc ($P \leq 0.001$); *Hgf* and *Ctgf* (connective tissue growth factor) are among the top 30 (Fig. 6B). *Hgf* and *Ctgf* are also among the top 30 of 305 up-regulated genes that are known to suppress apoptosis (Fig. 6B). In addition, IPA analysis revealed significant enrichment of eight canonical signaling pathways, including the Rho family GTPases, integrins, NFκB (nuclear factor kappa B), HGF, VEGF (vascular endothelial growth factor), WNT/β-catenin, STAT3 (signal transducer and activator of transcription 3), and ERK (extracellularly regulated kinase)/MAPK (p38 mitogen-activated protein kinases)
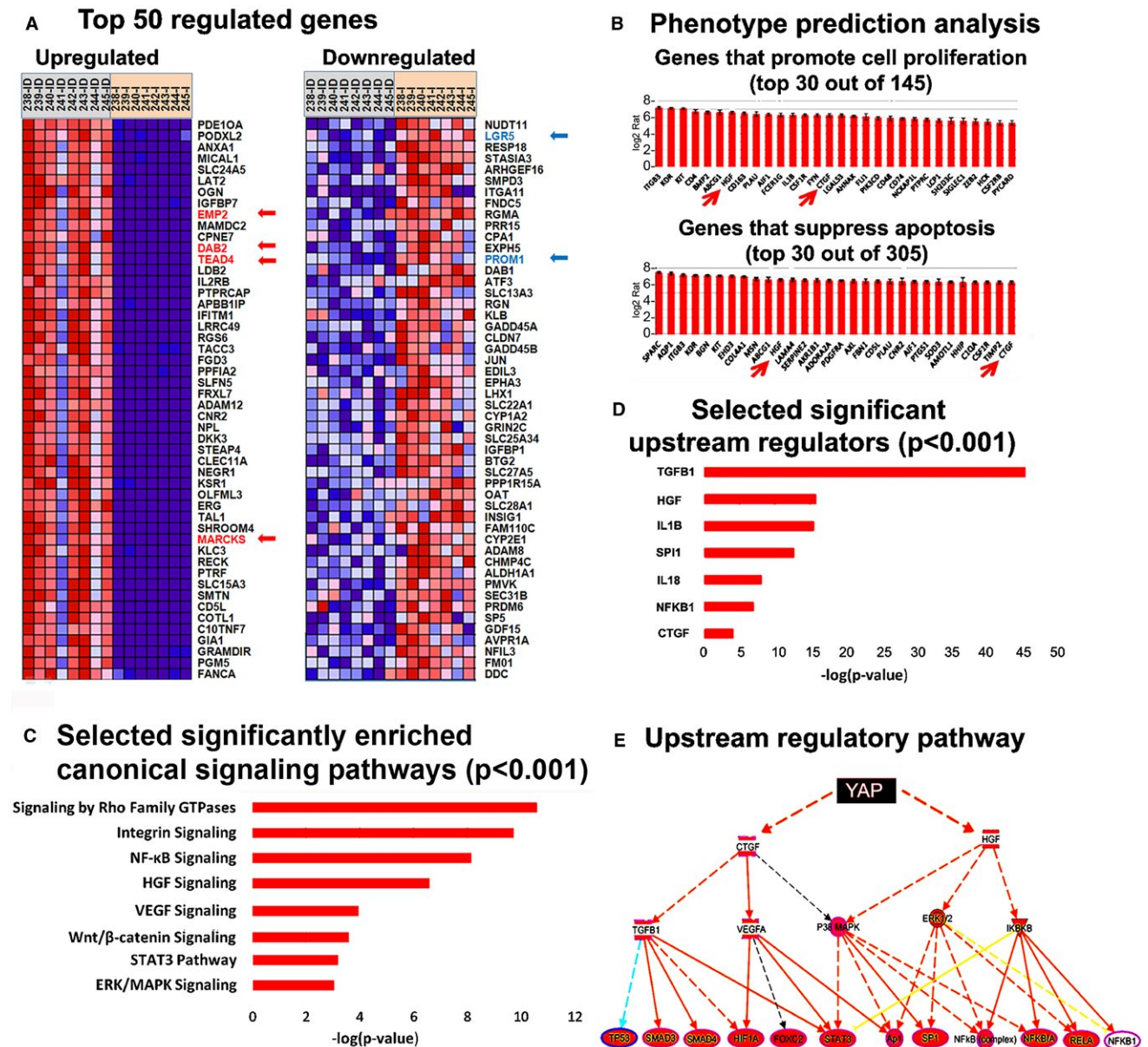
FIG. 6. GSEA and IPA analysis of RNAseq from ID/I pairs isolated at 3 months and 6 months following transplantation. (A) Heat map showing the top 50 most significantly up-regulated and down-regulated genes in ID/I pairs (red arrows, up-regulated genes specifically mentioned in text; blue arrows, down-regulated genes specifically mentioned in text). (B) Selected results from phenotype prediction analysis (IPA) identifying the top 30 genes in significantly enriched categories that promote cell proliferation and suppress apoptosis (red arrows highlight *Ctgf* and *Hgf,* which are among the top 30 genes in both categories). (C) Graph depicting significantly enriched canonical pathways identified using IPA. Shown are pathways with significantly positive Z scores and *P* values less than 0.001. Values shown are the log (*P* value) for each pathway. (D) Results of upstream regulator analysis (IPA) identifying upstream regulators that are significantly up-regulated in YAP-Hc with significantly positive Z scores and *P* values less than 0.001. (E) Putative gene network identified by upstream regulator analysis (IPA) that controls the cellular behavior of YAP-Hc during liver repopulation.

(Fig. 6C). Interestingly, although the WNT signaling pathway is significantly enriched, β-catenin is not up-regulated in YAP-Hc, due to increased expression of five inhibitors of WNT signaling, including *Dkk,*

Sfrp1, Apc, Sox, and *Rar* (Supporting Fig. S3). These pathways play important roles in controlling cell proliferation, migration, tissue remodeling and apoptosis, all of which are important for liver repopulation.

139

A

B

i. Donor Wistar-RHA

ii. Untreated Gunn rat

iii. No transduction/no tamoxifen

iv. Transduction + tamoxifen

v. Transduction/no tamoxifen

vi. Transduction/tamoxifen after 6m

C

i. H & E 20X

ii. UGT1A1 20X
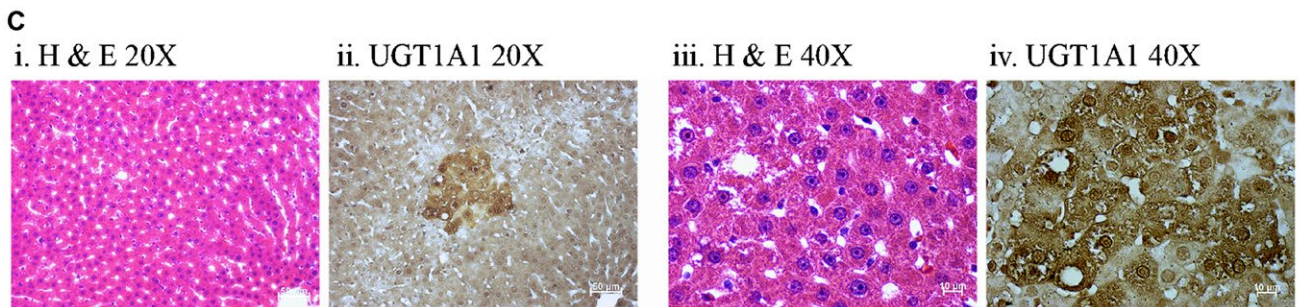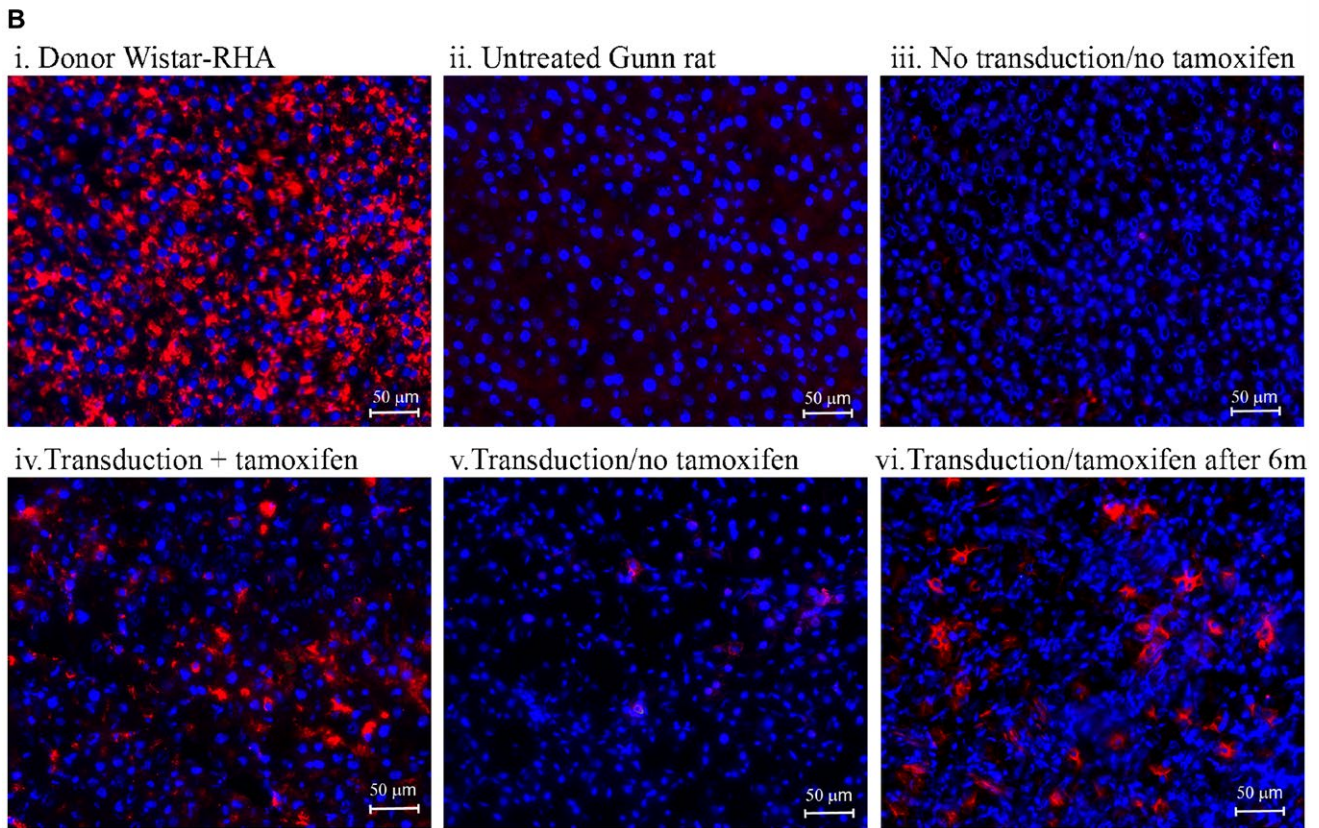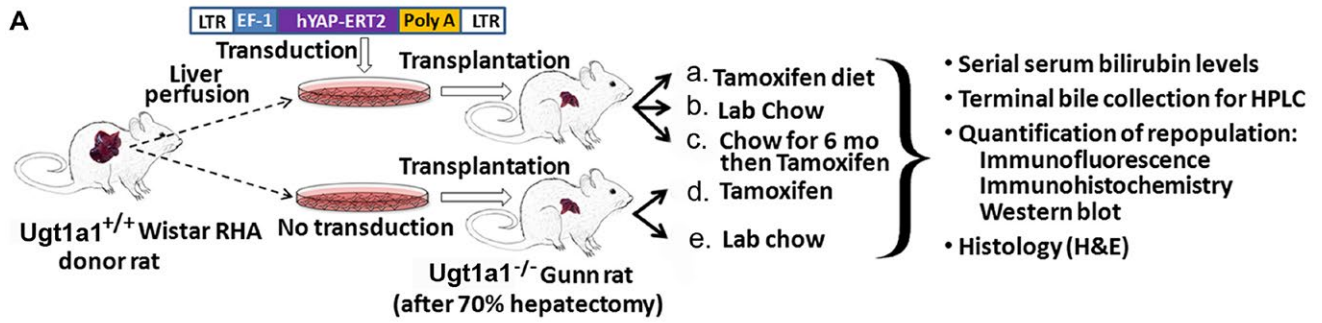
iii. H & E 40X

iv. UGT1A1 40X

FIG. 7. Gunn rat liver repopulation by transplanted Wistar-RHA rat hepatocytes. (A) Schematic diagram of five experimental Gunn rat groups: (a) transplanted with Wistar-RHA YAP-Hc followed by tamoxifen feeding; (b) similar to (a), but maintained on standard laboratory chow; (c) same as in (b), but switched to tamoxifen-containing diet after 6 months; (d) transplantation of nontransduced Wistar-RHA hepatocytes with tamoxifen feeding; and (e) transplantation of nontransduced Wistar-RHA hepatocytes, maintained on standard laboratory chow. (B) Immunofluorescence staining of rat liver sections for *Ugt1a1*: (i) Wistar-RHA donor rats; (ii) untreated Gunn rats, no transplantation; (iii) untreated Gunn rats, 8 months after transplanting nontransduced hepatocytes on standard lab chow; (iv) untreated Gunn rats, 8 months after transplanting Wistar-RHA YAP-Hc followed by tamoxifen feeding immediately after transplantation; (v) similar to (iv), but untreated Gunn rats maintained on standard lab chow; and (vi) similar to (v), but untreated Gunn rats switched to tamoxifen-containing diet 6 months after transplantation and followed for additional 6 months. (C) Normal liver histology and *Ugt1a1* staining: (i) consecutive liver sections from a Gunn rat in group B-iv stained with H&E at ×20 magnification; (ii) consecutive liver sections from a Gunn rat in group B-iv immunohistochemically stained for *Ugt1a1* at ×20 magnification; (iii) consecutive liver sections from a Gunn rat in group B-iv stained with H&E at ×40 magnification; and (iv) consecutive liver sections from a Gunn rat in group B-iv immunohistochemically stained for *Ugt1a1* at ×40 magnification. showed normal liver histology and *Ugt1a1* staining.

However, WNT signaling and β-catenin expression, which are up-regulated in hepatobiliary carcinogenesis,[28] are not up-regulated in our liver repopulation model, using hYAP-ERT2-transduced hepatocytes in a normal liver tissue microenvironment.

Finally, we used the upstream regulator prediction algorithm of IPA to identify potential upstream regulators that are significantly regulated by tamoxifen in YAP-Hc. These selected specific upstream regulators include *Tgfβ1* (transforming growth factor beta 1), *Hgf*, *Nfκb1*, and *Ctgf* (Fig. 6D). Using this analysis, we identified a network of regulators that represents a cascade of gene regulation, which may be important in control of the regenerative response induced by tamoxifen in YAP-Hc. In our data set, YAP-Hc show up-regulated *Hgf* and *Ctgf* signaling with cross-talk between Yap downstream regulators *Tgfβ1*, *Vegfa*, *p38 Mapk*, *Erk1/2* and *Iκbκb*, all of which up-regulate expression of specific genes affecting cell proliferation (Fig. 6E).

PREFERENTIAL PROLIFERATION OF WISTAR-RHA Yap-Hc TRANSPLANTED INTO GUNN RAT LIVERS

We evaluated the engraftment and proliferation of transplanted Wistar-RHA hepatocytes by immunofluorescence staining of liver sections for rat *Ugt1a1* and western blot analysis, using the experimental groups shown schematically in Fig. 7A. Hepatocytes in donor Wistar-RHA rats were positive for *Ugt1a1* (Fig. 7B-i), whereas hepatocytes in untreated Gunn rats were negative (Fig. 7B-ii). With transplanted nontransduced/nontamoxifen-treated Wistar-RHA hepatocytes, engrafted Ugt1a1⁺ cells were seen as single cells or doublets (Fig. 7B-iii). When Gunn rats were transplanted with YAP-Hc under continuous tamoxifen feeding, large clusters of Ugt1a1⁺ hepatocytes were produced (Fig. 7B-iv); such proliferation did not happen in the absence of tamoxifen (Fig. 7B-v). Interestingly, when we started tamoxifen feeding 6 months after YAP-Hc transplantation and continued tamoxifen for 6 more months, similar clusters of YAP-Hc were observed (Fig. 7B-vi).

REPOPULATED AREAS OF GUNN RAT LIVER WERE MORPHOLOGICALLY NORMAL

Repopulating YAP-Hc clusters in Gunn rat liver, stained with H&E or immunohistochemically for *Ugt1a1* in consecutive sections, were histologically normal (Fig. 7C-i,ii). At ×40 magnification (Fig. 7C-iii,iv), *Ugt1a1* staining in repopulating hepatocytes exhibited characteristic "clumpy," cytoplasmic distribution and enrichment in the nuclear envelope (Fig. 7C-iv), characteristic of its distribution in the endoplasmic reticulum.[29]

BOTH YAP-ERT2 TRANSDUCTION AND TAMOXIFEN ADMINISTRATION ARE REQUIRED TO INCREASE THE MASS OF DONOR-DERIVED Ugt1a1⁺ HEPATOCYTES

Western blots of liver homogenates with antibody against rat *Ugt1a1* showed an immunoreactive band of appropriate size in all Gunn rats that received hepatocyte transplantation (Fig. 8A), but was not found in

A

B

C

i. No cell transplantation

ii. No transduction no tamoxifen

iii. No transduction + tamoxifen

iv. Transduction, no tamoxifen

v. Transduction + tamoxifen

vi. Transduction, tamoxifen after 6 mo

D

i. Wistar-RHA rat

ii. Gunn rat: no cell transplantarion

iii. No transduction, no tamoxifen

iv. No transduction + tamoxifen

v. Transduction + tamoxifen

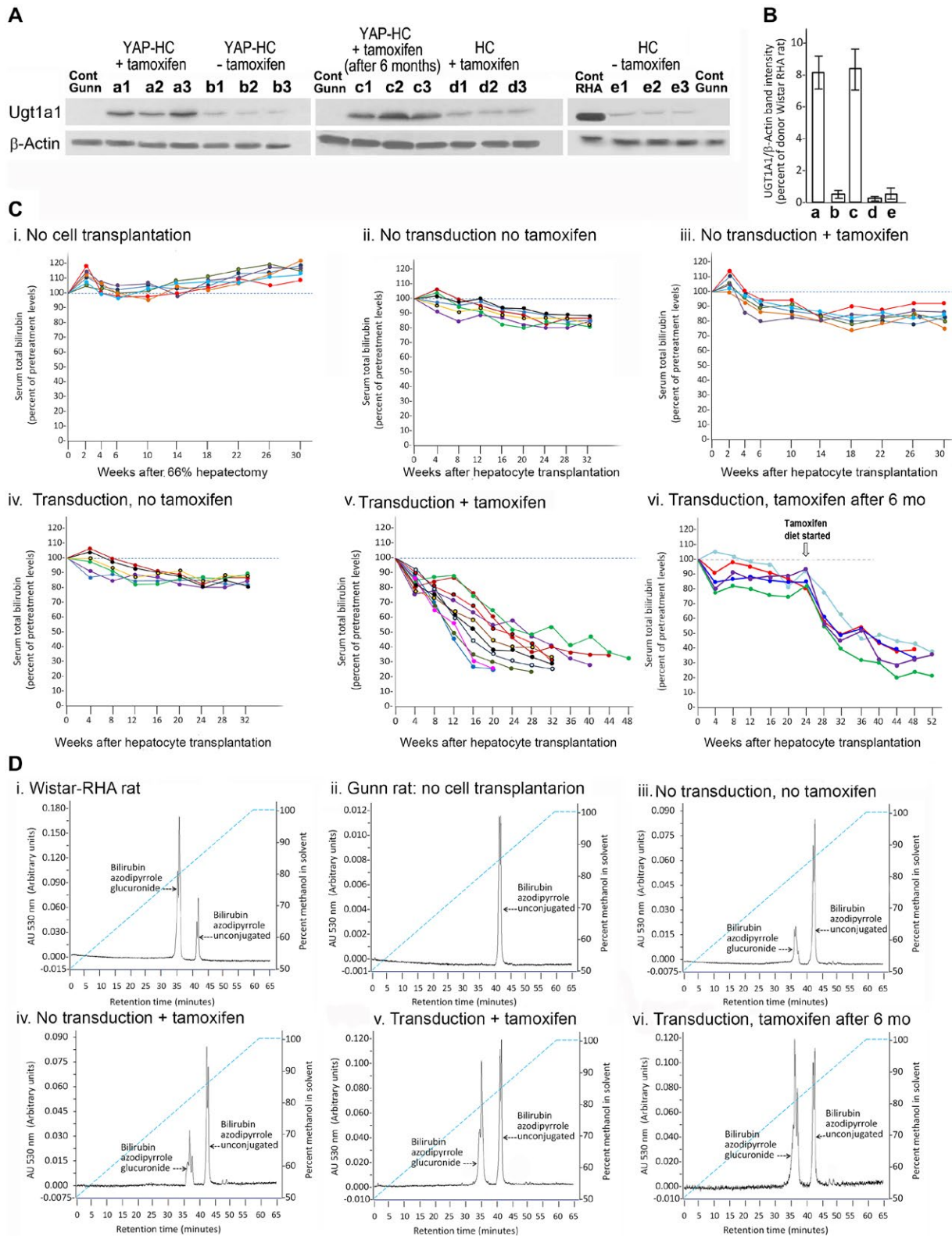vi. Transduction, tamoxifen after 6 mo

FIG. 8. Hepatic _Ugt1a1_ content and metabolic effect in recipient Gunn rats. (A) Western blots for _Ugt1a1_ in liver homogenates from Gunn rats: Each lane represents an individual rat (Cont, untreated Gunn rat; a1-a3, 7.5 months to 12 months after Wistar-RHA YAP-Hc transplantation; b1-b3, as in a1-a3 but maintained on standard lab chow; c1-c3, as in b1-b3 but tamoxifen diet started 6 months after transplantation; d1-d3, transplantation with nontransduced hepatocytes followed by tamoxifen feeding; e1-e3, as in d1-d3 but maintained on standard lab chow; RHA, liver homogenate of control Wistar-RHA rat (the amount of protein applied to this lane was 25% of that used for other lanes). (B) Relative abundance of _Ugt1a1_: The ratio between the band densities of _Ugt1a1_ and β-actin was determined for each lane and expressed as a percentage of the _Ugt1a1_/β-actin ratio observed for Wistar RHA rats. Bars a-e show the means ± SDs of rats in the corresponding groups in (A) (n = 3). (C) Serum bilirubin levels: Serum bilirubin was determined before and at various intervals after hepatocyte transplantation. Each line represents an individual recipient Gunn rat, and each dot is the mean of triplicate determinations. All Gunn rats underwent partial hepatectomy and then were grouped as follows: i, control Gunn rats without hepatocyte transplantation; ii, transplanted nontransduced hepatocytes, without tamoxifen feeding; iii, transplanted nontransduced hepatocytes followed by tamoxifen feeding; iv, transplanted Wistar-RHA YAP-Hc on standard lab chow; v, transplanted Wistar-RHA YAP-Hc on tamoxifen feeding; and vi, transplanted Wistar-RHA YAP-Hc switched to tamoxifen feeding 6 months after hepatocyte transplantation. (D) High-performance liquid chromatography of bilirubin in bile samples: Bilirubin species in bile samples obtained at sacrifice were converted to ethylanthranilate azodipyrroles (Supporting Information). Representative tracings from individual rats from the various groups are shown. Note that the scales (ordinate) are different for different samples: i, Wistar-RHA rat; ii, Gunn rat without cell transplantation; iii, Gunn rat transplanted with nontransduced hepatocytes, maintained on standard lab chow; iv, Gunn rat transplanted with nontransduced Wistar-RHA hepatocytes plus tamoxifen feeding; v, Gunn rat transplanted with Wistar-RHA YAP-Hc plus tamoxifen feeding; and vi, Gunn rat transplanted with Wistar-RHA YAP-Hc, maintained on standard lab chow for 6 months and then switched to tamoxifen feeding for 6 months.

---

nontransplanted Gunn rats (Fig. 8A, control Gunn lanes). β-Actin was used as internal control. The ratios of band intensities for _Ugt1a1_ and β-actin for each recipient Gunn rat liver was expressed as a percentage of that expressed in WT Wistar-RHA rats (Fig. 8B). Liver homogenates from Gunn rats transplanted with Wistar-RHA YAP-Hc and fed tamoxifen either immediately after transplantation (Fig. 8A, a1-a3), or beginning 6 months later (Fig. 8A, c1-c3), contained 8.25% ± 0.75% or 8.5% ± 0.8% of the _Ugt1a1_ present in WT Wistar-RHA rat livers (Fig. 8B, bars a and c, respectively). These levels were 17-fold to 35-fold greater than those found in Gunn rats that received YAP-Hc but no tamoxifen (Fig. 8A, b1-b3), nontransduced hepatocytes plus tamoxifen (Fig. 8A, d1-d3, and Fig. 8B, bars b and d, respectively), or hepatocytes without transduction or tamoxifen diet (Fig. 8A, e1-e3, and Fig. 8B, bar e), all with $P < 0.02$. These findings confirmed that expansion of transplanted Wistar-RHA YAP-Hc required both hYAP-ERT2 expression and its tamoxifen-induced nuclear translocation/function.

SERUM BILIRUBIN REDUCTION PARALLELS EXTENT OF LIVER REPOPULATION BY YAP-Hc

Gunn rats subjected to partial hepatectomy without hepatocyte transplantation exhibited increased serum bilirubin levels 2 weeks after partial hepatectomy, which resolved by 4 weeks, followed by a gradual age-related increase (Fig. 8C-i). All groups of Gunn rats transplanted with Wistar-RHA rat hepatocytes exhibited reduced serum bilirubin at time points beyond 16 weeks after transplantation (Fig. 8C-ii-vi). In rats transplanted with nontransduced Wistar-RHA hepatocytes without tamoxifen feeding (Fig. 8C-ii), with nontransduced Wistar-RHA hepatocytes plus tamoxifen (Fig. 8C-iii.), or with Wistar-RHA YAP-Hc but no tamoxifen (Fig. 8C-iv), long-term bilirubin reduction ranged from 8% to 20% (14% ± 6%). In contrast, rats that received Wistar-RHA YAP-Hc with tamoxifen administration starting immediately after cell transplantation showed a 65%-81% (73% ± 8%) serum bilirubin reduction (Fig. 8C-v): values that are significantly different from those in rats transplanted with Wistar-RHA YAP-Hc without tamoxifen administration (Fig. 8C-iv) ($P < 0.02$), or nontransduced hepatocytes with (Fig. 8C-iii) or without (Fig. 8C-ii) tamoxifen ($P < 0.02$). Interestingly, serum bilirubin was markedly reduced when tamoxifen feeding was initiated 6 months after transplantation of Wistar-RHA YAP-Hc (Fig. 8C-vi). After 20 to 24 weeks of tamoxifen administration, the hypobilirubinemic effect was similar to that attained by initiating tamoxifen feeding immediately after hepatocyte transplantation (Fig. 8C-v). These results confirm tight off/on control of YAP-ERT2 function by tamoxifen and indicate that engrafted YAP-Hc that had remained quiescent for a long time still retain proliferative responsiveness to tamoxifen.

HEPATOCYTE TRANSPLANTATION IN GUNN RATS RESULTED IN BILIARY EXCRETION OF BILIRUBIN GLUCURONIDE

We next collected bile samples before euthanasia and converted bilirubin species to ethylanthranilate azodipyrroles[30] for analysis by high-performance liquid chromatography (HPLC) (Supporting Information). As expected, the bile of WT Wistar-RHA rats yielded predominantly azodipyrrole glucuronides with a smaller amount of unconjugated azodipyrrole (Fig. 8D-i). Bile from Gunn rats that underwent partial hepatectomy without cell transplantation produced only unconjugated azodipyrroles (Fig. 8D-ii). Bile from Gunn rats receiving Wistar-RHA hepatocytes yielded both azodipyrrole glucuronide and unconjugated azodipyrrole (Fig. 8D-iii,vi). However, in rats receiving both Wistar-RHA YAP-Hc and tamoxifen, the area under the curve of azodipyrrole glucuronides was much increased and equaled that of unconjugated azodipyrroles (Fig. 8D-v,vi). These findings independently confirmed a far greater repopulation of Gunn rat livers transplanted with Wistar-RHA YAP-Hc plus tamoxifen, compared with control Wistar-RHA hepatocytes, and demonstrated normal physiologic function of these cells in Gunn rats.

Discussion

We show that repopulation of normal rat liver by YAP-Hc is tightly controlled by tamoxifen feeding. Repopulation was increased 4-fold between 6 months and 12 months, demonstrating long-term proliferation of engrafted cells. Proliferating donor hepatocytes appeared morphologically normal, with normal cellular polarity and orientation within the hepatic plates without distortion or compression of surrounding parenchyma and without evidence of fibrosis, increased aneuploidy, or neoplastic transformation. Studies in Gunn rats showed that the bilirubin lowering effect of transplanted YAP-Hc was markedly enhanced (mean 73% reduction) only when tamoxifen was administered. Although serum bilirubin concentrations did not decline to levels in WT control rats, if the same percent reduction could be achieved in CN1 patients, this would represent a major therapeutic benefit, as the risk of kernicterus would be removed without the need for phototherapy.

Mature hepatocytes transplanted into the liver through the portal venous system engraft in the liver as single cells or in small groups of 2 to 3 cells. In recipients without chronic liver injury, these cells undergo minimal proliferation even in response to 66% partial hepatectomy, because host hepatocytes proliferate in parallel with donor hepatocytes. Thus, liver repopulation by transplanted cells depends on the balance between the proliferative potential and apoptotic behavior of host versus transplanted hepatocytes. Such competitive advantage for engrafted normal adult hepatocytes may preexist in some genetic diseases, such as hereditary tyrosinemia or α_1-antitrypsin deficiency, in which host hepatocytes are undergoing chronic injury.[7] However, there is no underlying hepatocellular injury in many monogenic liver diseases. Here we present a strategy that permits repopulation of host livers in a normal tissue microenvironment by providing donor cells with a pharmacologically controlled cell-intrinsic proliferative and survival advantage over host hepatocytes. At both 6 months and 12 months after cell transplantation, donor cell clusters contained significantly more Ki67-positive dividing cells and significantly fewer caspase 3–positive apoptotic cells (Fig. 4), indicating that enhanced proliferation and reduced cell death, the basic features of cell competition, are responsible for liver repopulation by YAP-Hc.

A major concern in studies that increase the proliferative activity of transplanted cells is associated tumor risk. In a study of liver cell fate, Yimlamai et al.[31] noted that Yap expression was much higher in biliary epithelial cells than in adult hepatocytes, and when Yap expression in transgenic hepatocytes was induced by doxycycline, mature hepatocytes dedifferentiated, hepatobiliary progenitor genes were turned on, and the cells differentiated along the biliary lineage. High Yap expression favored a biliary phenotype; therefore, it was concluded that different Yap levels/activity could determine different hepatic cell fates.[31] Based on similar reasoning, we expressed hYAP-ERT2 under the TTR promoter, which is hepatocyte-specific and weaker than the TRE (tetracycline response element) promoter used by Yimlamai et al.,[31] and our experiments were performed in a normal liver microenvironment. Both of these factors could contribute to the lack of hepatobiliary transdifferentiation.

Other interesting findings revealed by RNAseq are that (1) *Lrg5*, a marker for stem and progenitor cells in many tissues including the liver,[26] is not hyperexpressed in repopulating hepatocytes; (2) *Hgf* and C*tgf* are among the top 30 up-regulated cell proliferation and antiapoptotic genes in YAP-Hc; (3) YAP-Hc exhibit a Yap signature; (4) *Tead4*, which is in a signaling pathway that activates a potent liver tumor suppressor, *Dlc1*, a tumor-suppressor gene,[20-24] was highly up-regulated (12.8 fold); and (5) both *Tns3*, a downstream Yap target, and *Dlc1*, which is activated by *Tns3* binding, are up-regulated in YAP-Hc. Several other tumor-suppressor genes in the cancer genome landscape,[25] *Prdm1, Kdm6a, Tnfa1P3, Atm* and *Msh2,* are also significantly up-regulated in repopulating YAP-Hc. Finally, increased IHH expression, which is required for EMT and hepatic fibrosis,[22] was not hyperexpressed in YAP-Hc (Fig. 5E). Overall, these findings provide a molecular explanation for the absence of dedifferentiation, hepatic progenitor cell formation, hepatobiliary transformation, EMT, fibrosis, or carcinogenesis in our repopulation model. Furthermore, YAP/TAZ activation can induce negative feedback to regulate Hippo pathway homeostasis,[32] which could, conceivably, limit the effect of tamoxifen-activated YAP-Hc. If true, tamoxifen-activated YAP-ERT2 would be sufficient for liver repopulation by YAP-Hc but not for hepatocarcinogenesis.

Expression of HGF, an important cytokine in liver regeneration,[33] is regulated in YAP-Hc, an interesting new finding that will require further study. We also found that several canonical signaling pathways that are important for control of cell behavior, including migration, remodeling, cell proliferation and apoptosis, are significantly enriched among the genes up-regulated in YAP-Hc (Fig. 6C). This, accompanied by identification of a network of upstream regulators (Fig. 6D,E), provides insight into how a small but continuous competitive advantage of YAP-Hc can lead to effective replacement of host hepatocytes with restoration of liver function, as demonstrated by the marked reduction of serum bilirubin in the Gunn rat model of CN1 (Fig. 8C,D).

In summary, our cell transplantation strategy enables long-term repopulation of livers without pre-existing or induced liver injury. Repopulation is under tight pharmacological control and is not associated with distortion of liver architecture, hepatocyte dedifferentiation, transdifferentiation, EMT, or neoplastic transformation. With further development, this strategy could be useful in treating a large number of inherited metabolic disorders of the liver that are not associated with chronic liver injury.

REFERENCES

1) Moini M, Mistry P, Schilsky ML. Liver transplantation for inherited metabolic disorders of the liver. Curr Opin Organ Transplant 2010;15:269-276.

2) Jorns C, Ellis EC, Nowak G, Fischler B, Nemeth A, Strom SC, et al. Hepatocyte transplantation for inherited metabolic diseases of the liver. J Intern Med 2012;272:201-223.

3) Laconi E, Oren R, Mukhopadhyay DK, Hurston E, Laconi S, Pani P, et al. Long-term, near-total liver replacement by transplantation of isolated hepatocytes in rats treated with retrorsine. Am J Pathol 1998;153:319-329.

4) Guha C, Sharma A, Gupta S, Alfieri A, Gorla GR, Gagandeep S, et al. Amelioration of radiation-induced liver damage in partially hepatectomized rats by hepatocyte transplantation. Cancer Res 1999;59:5871-5874.

5) Rhim JA, Sandgren EP, Degen JL, Palmiter RD, Brinster RL. Replacement of diseased mouse liver by hepatic cell transplantation. Science 1994;263:1149-1152.

6) Overturf K, Al-Dhalimy M, Tanguay R, Brantly M, Ou CN, Finegold M, et al. Hepatocytes corrected by gene therapy are selected in vivo in a murine model of hereditary tyrosinaemia type I. Nat Gen 1996;12:266-273.

7) Ding J, Yannam GR, Roy-Chowdhury N, Hidvegi T, Basma H, Rennard SI, et al. Spontaneous hepatic repopulation in transgenic mice expressing mutant human alpha1-antitrypsin by wild-type donor hepatocytes. J Clin Invest 2011;121:1930-1934.

8) Malhi H, Irani AN, Volenberg I, Schilsky ML, Gupta S. Early cell transplantation in LEC rats modeling Wilson's disease eliminates hepatic copper with reversal of liver disease. Gastroenterology 2002;122:438-447.

9) Witek RP, Fisher SH, Petersen BE. Monocrotaline, an alternative to retrorsine-based hepatocyte transplantation in rodents. Cell Transplant 2005;14:41-47.

10) Sandhu JS, Petkov PM, Dabeva MD, Shafritz DA. Stem cell properties and repopulation of the rat liver by fetal liver epithelial progenitor cells. Am J Pathol 2001;159:1323-1334.

11) **Yovchev M**, **Jaber FL**, Lu Z, Patel S, Locker J, Rogler LE, et al. Experimental model for successful liver cell therapy by lenti TTR-YapERT2 transduced hepatocytes with tamoxifen control of Yap subcellular location. Sci Rep 2016;6:19275.

12) Pan D. The hippo signaling pathway in development and cancer. Dev Cell 2010;19:491-505.

13) Johnson R, Halder G. The two faces of Hippo: targeting the Hippo pathway for regenerative medicine and cancer treatment. Nat Rev Drug Discov 2014;13:63-79.

14) Ogawa K, Medline A, Farber E. Sequential analysis of hepatic carcinogenesis: the comparative architecture of preneoplastic, malignant, prenatal, postnatal and regenerating liver. Br J Cancer 1979;40:782-790.

15) Moreno E, Basler K. dMyc transforms cells into super-competitors. Cell 2004;117:117-129.

16) **Mootha VK**, **Lindgren CM**, Eriksson KF, Subramanian A, Sihag S, Lehar J, et al. PGC-1alpha-responsive genes involved in oxidative phosphorylation are coordinately downregulated in human diabetes. Nat Genet 2003;34:267-273.

17) **Subramanian A**, **Tamayo P**, Mootha VK, Mukherjee S, Ebert BL, Gillette MA, et al. Gene set enrichment analysis: a knowledge-based approach for interpreting genome-wide expression profiles. Proc Natl Acad Sci U S A 2005;102:15545-15550.

18) Zhang J, Smolen GA, Haber DA. Negative regulation of YAP by LATS1 underscores evolutionary conservation of the Drosophila Hippo pathway. Cancer Res 2008;68:2789-2794.

19) Cordenonsi M, Zanconato F, Azzolin L, Forcato M, Rosato A, Frasson C, et al. The Hippo transducer TAZ confers cancer stem cell-related traits on breast cancer cells. Cell 2011;147:759-772.

20) Hansen CG, Ng YL, Lam WL, Plouffe SW, Guan KL. The Hippo pathway effectors YAP and TAZ promote cell growth by modulating amino acid signaling to mTORC1. Cell Res 2015;25:1299-1313.

21) Park YY, Sohn BH, Johnson RL, Kang MH, Kim SB, Shim JJ, et al. Yes-associated protein 1 and transcriptional coactivator with PDZ-binding motif activate the mammalian target of rapamycin complex 1 pathway by regulating amino acid transporters in hepatocellular carcinoma. Hepatology 2016;63:159-172.

22) Wang X, Zheng Z, Caviglia JM, Corey KE, Herfel TM, Cai B, et al. Hepatocyte TAZ/WWTR1 promotes inflammation and fibrosis in nonalcoholic steatohepatitis. Cell Metab 2016;24:848-862.

23) Zhou X, Thorgeirsson SS, Popescu NC. Restoration of DLC-1 gene expression induces apoptosis and inhibits both cell growth and tumorigenicity in human hepatocellular carcinoma cells. Oncogene 2004;23:1308-1313.

24) Cao X, Voss C, Zhao B, Kaneko T, Li SS. Differential regulation of the activity of deleted in liver cancer 1 (DLC1) by tensins controls cell migration and transformation. Proc Natl Acad Sci U S A 2012;109:1455-1460.

25) Vogelstein B, Papadopoulos N, Velculescu VE, Zhou S, Diaz LA Jr, Kinzler KW. Cancer genome landscapes. Science 2013;339:1546-1558.

26) **Huch M**, **Dorrell C**, Boj SF, van Es JH, Li VS, van de Wetering M, et al. In vitro expansion of single Lgr5+ liver stem cells induced by Wnt-driven regeneration. Nature 2013;494:247-250.

27) Li Z. CD133: a stem cell biomarker and beyond. Exp Hematol Oncol 2013;2:17.

28) Monga SP. b-Catenin signaling and roles in liver homeostasis, injury and tumorigenesis. Gastroenterology 2015;148: 1294-1310.

29) Chowdhury JR, Novikoff PM, Chowdhury NR, Novikoff AB. Distribution of UDPglucuronosyltransferase in rat tissue. Proc Natl Acad Sci U S A 1985;82:2990-2994.

30) Trotman BW, Roy-Chowdhury J, Wirt GD, Bernstein SE. Azodipyrroles of unconjugated and conjugated bilirubin using diazotized ethyl anthranilate in dimethyl sulfoxide. Anal Biochem 1982;121:175-180.

31) **Yimlamai D**, **Christodoulou C**, Galli GG, Yanger K, Pepe-Mooney B, Gurung B, et al. Hippo pathway activity influences liver cell fate. Cell 2014;157:1324-1338.

32) Moroishi T, Park HW, Qin B, Chen Q, Meng Z, Plouffe SW, et al. A YAP/TAZ-induced feedback mechanism regulates Hippo pathway homeostasis. Genes Dev 2015;29:1271-1284.

33) Michalopoulos GK, DeFrancesMC. Liver regeneration. Science 1997;276:60-66.

Author names in bold designate shared first authorship.

Supporting Information

Additional Supporting Information may be found at onlinelibrary.wiley.com/doi/10.1002/hep4.1278/suppinfo.